PLANAR AND POLY-ARC LOMBARDI DRAWINGS*

Christian A. Duncan,† *David Eppstein,*‡ *Michael T. Goodrich,*‡ *Stephen G. Kobourov,*§ *Maarten Löffler,*¶ *Martin Nöllenburg*‖

Abstract. In Lombardi drawings of graphs, edges are represented as circular arcs and the edges incident on vertices have perfect angular resolution. It is known that not every planar graph has a planar Lombardi drawing. We give an example of a planar 3-tree that has no planar Lombardi drawing and we show that all outerpaths do have a planar Lombardi drawing. Further, we show that there are graphs that do not even have any Lombardi drawing at all. With this in mind, we generalize the notion of Lombardi drawings to that of (smooth) k-Lombardi drawings, in which each edge may be drawn as a (differentiable) sequence of k circular arcs; we show that every graph has a smooth 2-Lombardi drawing and every planar graph has a smooth planar 3-Lombardi drawing. We further investigate related topics connecting planarity and Lombardi drawings.

1 Introduction

Motivated by the work of the American abstract artist Mark Lombardi [28], who specialized in drawings that illustrate financial and political networks (see Figures 1 and 2), Duncan et al. [15, 16] proposed a graph visualization style called *Lombardi drawings*. These types of drawings attempt to capture some of the visual aesthetics used by Mark Lombardi, including his use of circular-arc edges and well-distributed edges around each vertex.

A vertex with circular arc edges extending from it has *perfect angular resolution* if the smaller of the two angles between any two consecutive edges, as measured between the tangents to the circular arcs at the vertex, all have the same (arc) degree. A *Lombardi drawing* of a graph $G = (V, E)$ is a drawing of a graph where every vertex is represented as a point, the edges incident to each vertex have perfect angular resolution, and every edge is represented as a circular arc or a line segment (i.e., a circular arc of infinite radius) between the points associated with the incident vertices of the edge.

*Preliminary results contained in this paper appeared in Graph Drawing 2011 [14] and Graph Drawing 2012 [29]. This research was supported in part by the National Science Foundation under grants 0830403, CCF-1423411, and CCF-1712119, by the Office of Naval Research under MURI grant N00014-08-1-1015, by the German Research Foundation under grant NO 899/1-1, and by the Dutch National Science Foundation (NWO) under grant 639.021.123.

†*Dept. of Engineering, Quinnipiac University, Hamden, CT, USA*, christian.duncan@quinnipiac.edu

‡*Dept. of Computer Science, University of California, Irvine, CA, USA*, eppstein@ics.uci.edu, goodrich@acm.org

§*Dept. of Computer Science, University of Arizona, Tucson, AZ, USA*, kobourov@cs.arizona.edu

¶*Dept. of Information and Computing Sciences, Utrecht University, NL*, m.loffler@uu.nl

‖*Algorithms and Complexity Group, TU Wien, Vienna, AT*, noellenburg@ac.tuwien.ac.at

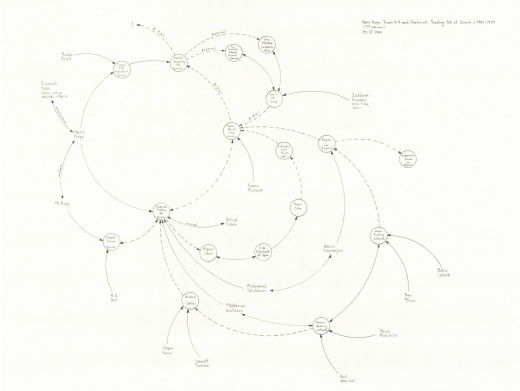

Figure 1: Mark Lombardi, *Hans Kopp, Trans K-B and Shakarchi Trading AG of Zurich, ca. 1981–89* (3rd Version), 1999, 20.25 × 30.75 inches (cat. no. 22) [28]. Image courtesy Pierogi Gallery and the Lombardi Family.

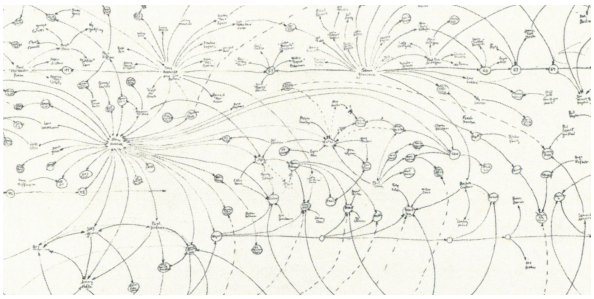

Figure 2: Clipping of Mark Lombardi, *Chicago Outfit and Satellite Regimes, ca. 1931–83*, 1998, 48.125 × 96.6225 inches (cat. no. 11) [28]. Image Courtesy Pierogi Gallery and the Lombardi Family. Private Collection.

One drawback of previous work on Lombardi drawings is that not every graph has a Lombardi drawing. In this paper we attempt to remedy this by considering drawings in which edges are represented by poly-arcs, i.e., sequences of circular arcs. This added generality will allow us to draw any graph.

Drawing planar graphs without crossings is a natural goal for graph drawing algorithms, and one that is easy to achieve when angular resolution is ignored. Lombardi himself avoided crossings in many of his drawings, as shown in Figure 1. We say that a graph is *planar Lombardi* if it has a planar Lombardi drawing. Interestingly, there are planar graphs that are not planar Lombardi [15, 18] and an immediate question is to characterize those planar graphs that are planar Lombardi. For example, it is known that trees [16], Halin graphs [15] and their generalizations called D3-reducible graphs [19], subcubic planar graphs and some (but not all) 4-regular graphs [18] are planar Lombardi. Here we continue the investigation of planar Lombardi drawings. A well-studied subclass of planar graphs are outerplanar graphs, but in terms of Lombardi drawings it remains open whether all outerplanar graphs are planar Lombardi. In this paper we show that all *outerpaths*, i.e., outerplanar graphs whose weak dual is a path, are planar Lombardi. Moreover, we extend our investigations to the planarity of poly-arc Lombardi drawings.

We define a *k-Lombardi drawing* to be a poly-arc drawing with at most k circular arcs per edge, with a 1-Lombardi drawing being equivalent to the earlier definition of a Lombardi drawing. We say that a k-Lombardi drawing is *smooth* if every edge is continuously differentiable, i.e., no edge in the drawing has a sharp bend. If a k-Lombardi drawing is not smooth, we say it is *pointed*. Fortunately, we do not need large values of k to be able to draw all graphs: as we show, every graph has a smooth 2-Lombardi drawing. Interestingly, this result is hinted at in the work of Lombardi himself—Figure 2 shows a portion of a drawing

by Lombardi that uses smooth edges consisting of two near-circular arcs.

New Results. In this paper we provide the following results:

- We prove that every outerpath is planar Lombardi. However, we find examples of planar 3-trees with no planar Lombardi drawing, strengthening an example from [15] of a planar graph with treewidth greater than three that is not planar Lombardi. These results are described in Section 3.
- We find examples of graphs that do not have a Lombardi drawing, regardless of the ordering of edges around each vertex, thus strengthening an example from [15] of graphs for which a specific edge ordering cannot be drawn. In contrast, we show how to construct a smooth 2-Lombardi drawing for any graph. These results are described in Section 4.
- We show how to represent any planar graph with a pointed 2-Lombardi planar drawing or a smooth 3-Lombardi planar drawing. These results are described in Section 5.

Related Work. In addition to the earlier theoretical work on Lombardi drawings discussed above, there is considerable prior work on graph drawing with circular-arc or curvilinear edges for the sake of achieving good, but not necessarily perfect, angular resolution [10, 23]. Confluent drawings, which use a crossing-free system of smooth arcs and junctions (similar to train tracks) to represent non-planar graphs, have been introduced by Dickerson et al. [13]. In a confluent drawing, two vertices are connected if and only if there exists a smooth, locally monotone path between them through this system of arcs and junctions. Similarly, edge bundling [27] refers to a set of heuristic techniques used in network visualization to reduce visual clutter by spatially grouping edges with similar geometric or structural properties as smooth curves. Both techniques, however, do not aim at optimizing angular resolution, but to the contrary use curvilinear arcs for merging individual edges at angles of 0°.

Brandes and Wagner [9] provided a force-directed algorithm for visualizing train schedules using Bézier curves for edges and fixed positions for vertices. Finkel and Tamassia [21] extended this work by giving a force-directed method for drawing graphs with curvilinear edges where vertex positions are not fixed. Aichholzer et al. [1] showed, for a given embedded planar triangulation with fixed vertex positions, it is possible to find a circular-arc drawing that maximizes the minimum angular resolution by solving a linear program. Chernobelskiy et al. [11] described functional Lombardi force-directed schemes, which are based on the use of dummy vertices and tangent forces, but may not always achieve perfect angular resolution. Interestingly, Efrat et al. [17] showed that, given a fixed placement of the vertices of a planar graph, it is NP-complete to determine whether the edges can be drawn with circular arcs so that there are no crossings. Thus, to the best of our knowledge, none of this related work correctly results in drawings of graphs having perfect angular resolution and curvilinear edges.

Graph layouts representing edges as circular or curvilinear arcs have also been investigated from a user's perspective. Two studies compared straight-line drawings with

circular-arc or curvilinear drawings [31, 32] but remained inconclusive in their findings; the former reports aesthetic preference for Lombardi-like layouts but worse task performance, while the latter study reports aesthetic preference for straight-line drawings. A study by Huang et al. [25] investigated the effects of curves on graph perception, when curved arcs are used to reduce edge crossings.

Alternatively, some previous work achieves good angular resolution using straight-line drawings [12, 22, 30] or piecewise-linear poly-arc drawings [20, 24, 26]. Di Battista and Vismara [12] characterized straight-line drawings of planar graphs with a prescribed assignment of angles between consecutive edges incident on the same vertex.

Bekos et al. [8] proposed smooth orthogonal drawings, in which every edge is a sequence of axis-aligned segments and circular arc segments with common axis-aligned tangents. Such drawings are a combination of orthogonal graph layouts and Lombardi drawings as vertices have an angular resolution of 90° and edges are either straight-line segments or quarter/half/three-quarter arc segments. Alam et al. [2] described an algorithm for planar graphs with maximum degree 4 that constructs smooth orthogonal drawings with edge complexity 2, which matches the corresponding lower bound. Bekos et al. [7] showed how to obtain bendless smooth orthogonal drawings for the subclass of planar graphs of maximum degree 3. Recently, Bekos et al. [6] showed NP-hardness for a restricted version of the bendless drawing problem for smooth orthogonal drawing and Argyriou et al. [4] studied the curve complexity of 1-plane smooth orthogonal drawings, i.e., drawings with at most one crossing per edge.

2 Preliminaries

In a Lombardi drawing, each vertex v has $\deg(v)$ outgoing edges equally spaced around v. We denote the tangent vector of any such edge as the *stub* of that edge. Further, a *k-degenerate graph* is a graph that can be reduced to the empty graph by iteratively removing vertices of degree at most k.

Before establishing our main results, we review several useful geometric properties related to Lombardi drawings and circular arcs. We begin by reviewing two key properties partially established by Duncan et al. [15]:

Property 1 ([15], Property 1)**.** Let A be a circular arc or line segment connecting two points p and q that both lie on circle O. Then A makes the same angle to O at p that it makes at q. Moreover, for any p and q on O and any angle $0 \leq \theta \leq \pi$, there exist either two arcs or a line segment and pair of collinear rays connecting p and q, making angle θ with O, one lying inside and one outside of O.

Property 2 ([15], Property 2)**.** Suppose we are given two points $p = (p_x, p_y)$ and $q = (q_x, q_y)$ and associated angles θ_{ph} and θ_{qh} and an angle θ_{pq}. Consider all pairs of circular arcs that leave p and q with angles θ_{ph} and θ_{qh} respectively (measured with respect to the positive horizontal axis) and meet at an angle θ_{pq} in a point. The locus of meeting points for these pairs of arcs is a circle C. Moreover, the circle C has radius $r_c = d_{pq} \csc \alpha/2$ and center $(p_x + r_c \sin(\alpha+\beta), p_y - r_c \cos(\alpha+\beta))$, where $\alpha = (\theta_{ph} - \theta_{qh} - \theta_{pq})/2$, β is the angle formed by

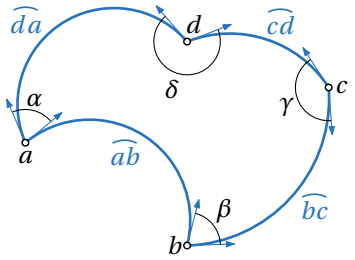

Figure 3: An arc quadrilateral $\diamondsuit abcd$.

the ray from p through q with respect to the positive horizontal axis, and d_{pq} is the distance between the points p and q.

Proof. The first part of this property was established by Duncan et al. [15]. Hence, for the remainder of the proof concerning the radius of C, we assume the reader is familiar with the arguments by Duncan et al. [15]. For simplicity at the moment, let us assume that p and q are aligned horizontally, that is $\beta = 0$. Let C represent the circular locus with center $c = (x_c, y_c)$ and radius r_c. From [15] we know that the angle formed by the center of the circle and the two points q and p is $\angle qcp = \theta_{ph} - \theta_{qh} - \theta_{pq} = 2\alpha$. Analyzing the isosceles triangle $\triangle qcp$, we determine the radius $r_c = d_{pq}/(2\sin\alpha)$.

Now, if $\beta \neq 0$, a simple rotation of $-\beta$ about p can be applied yielding $\alpha = \theta_{ph} - \beta - \theta_{qh} + \beta - \theta_{pq}$ and hence the angle α and the radius r_c are unaffected.

Using basic trigonometry and geometry, we can also determine the center of this circle as $c = (p_x + r_c \sin(\alpha+\beta), p_y - r_c\cos(\alpha+\beta))$. □

We denote the circle C of Property 2 as the *placement circle* of a new vertex with respect to its neighbors p and q and the angle θ_{pq}. An *arc quadrilateral* is a cycle consisting of four points in $\mathbb{R}^2$, and four arcs connecting the points. We say an arc quadrilateral is *planar* if the arcs only intersect at the points. We denote the points by a, b, c, and d, and the arcs by $\widehat{ab}$, $\widehat{bc}$, $\widehat{cd}$, and $\widehat{da}$. Let α be the angle at a between $\widehat{da}$ and $\widehat{ab}$, measured counter-clockwise. Similarly, let β be the angle at b between $\widehat{ab}$ and $\widehat{bc}$, let γ be the angle at c between $\widehat{bc}$ and $\widehat{cd}$, and let δ be the angle at c between $\widehat{cd}$ and $\widehat{da}$. Figure 3 shows an example.

Property 3. Let $\diamondsuit abcd$ be an arc quadrilateral. Then a, b, c, and d are concyclic iff $\alpha + \gamma - \beta - \delta = 0 \mod 360°$.

Proof. Let $\sigma = \alpha + \gamma - \beta - \delta$. Observe that if we change the radius of an arc, say $\widehat{ab}$, while keeping a and b fixed, α and β change by the same amounts. Therefore, σ is invariant under this operation unless a pair of arcs changes order. When an order change does occur, α (or β) either changes from 0° to 360° or from 360° to 0°. Therefore, $\sigma \mod 360°$ is invariant under any radius changes. Now, change the radii of all arcs until we obtain a straight-edge quadrilateral $\square abcd$. If $\square abcd$ is planar, it is well-known that a, b, c, and d are concyclic iff $\alpha + \gamma = 180°$. Since in this case $\alpha + \beta + \gamma + \delta = 360°$, the claim follows. If $\square abcd$

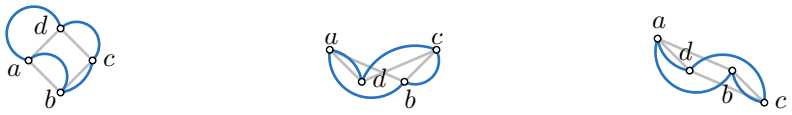

(a) (b) (c)

Figure 4: (a) An arc quadrilateral without flips. (b) An arc quadrilateral with one flip. (c) An arc quadrilateral with two flips.

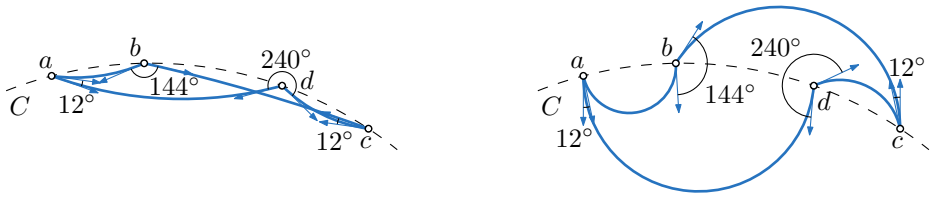

(a) (b)

Figure 5: If $\sigma = 360°$, then a, b, c, and d are concyclic on C. Therefore, the arcs need to be on opposite sides of C to make a planar drawing. (a) A non-planar arc quadrilateral. (b) A planar arc quadrilateral.

is not planar, assume w.l.o.g. $\overline{ab}$ and $\overline{cd}$ cross. In this case, a, b, c, and d are concyclic iff $\alpha + \gamma = \beta + \delta = 360°$; again the claim follows. □

Let $Q = \diamondsuit abcd$ be a simple arc quadrilateral whose vertices are labeled a, b, c, d in counterclockwise order. Let P be the straight-edge quadrilateral $\square abcd$. Then P could have the same orientation as Q, be non-simple, or have reversed orientation, see Figure 4.

Property 4. Let α, β, γ, and δ be four angles such that $\sigma = \alpha + \gamma - \beta - \delta < 360°$. Let a, b, and c be three points in the plane on a circle C, and let $\overset{\frown}{ab}$ and $\overset{\frown}{bc}$ be two arcs that meet at b at an angle of β such that $\overset{\frown}{ab}$ and $\overset{\frown}{bc}$ lie on the same side of C. Then the placement arc for d such that the four angles satisfy their specification lies on the same side of C as $\overset{\frown}{ab}$ and $\overset{\frown}{bc}$. Furthermore, there is a placement of d that results in a planar arc quadrilateral $\diamondsuit abcd$.

Proof. Let $\sigma = \alpha + \gamma - \beta - \delta$. By Property 2, there is a circle of possible placements for d that satisfies the angle constraints given by α and γ. If $\sigma = 360°$, by Property 3, this circle is C. If $\overset{\frown}{ab}$ and $\overset{\frown}{bc}$ are on the same side of C, then so are $\overset{\frown}{cd}$ and $\overset{\frown}{da}$. Figure 5(a) illustrates this situation and $\diamondsuit abcd$ is non-planar for any placement of d. (Note that if $\overset{\frown}{ab}$ and $\overset{\frown}{bc}$ are on different sides of C, then a planar arc quadrilateral $\diamondsuit abcd$ exists, see Figure 5(b).) Now if $\sigma < 360°$, the placement circle C' of d is different from C and C' and C intersect in points a and c. Figure 6 depicts the situation. Placing d on C' in between the two arcs $\overset{\frown}{ab}$ and $\overset{\frown}{bc}$ results in a planar arc quadrilateral $\diamondsuit abcd$. □

3 Planar Lombardi Drawings

In this section, we investigate *planar* (non-crossing) Lombardi drawings.

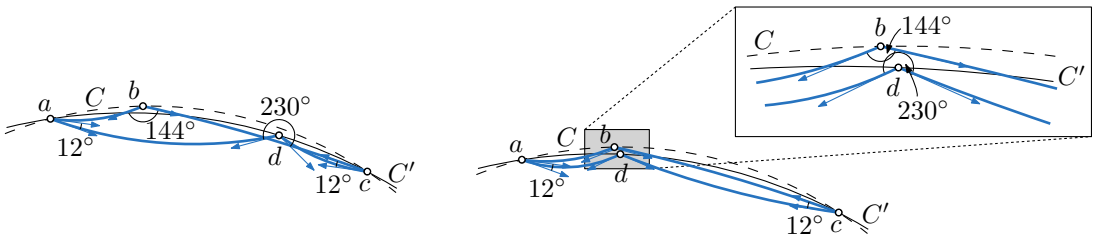

Figure 6: If $\sigma < 360°$, then the placement circle C' for d intersects C in a and c. (a) For some positions of d on C' the arc quadrilateral remains non-planar. (b) If d is placed on C' in between the arcs $\widehat{ab}$ and $\widehat{bc}$ the arc quadrilateral becomes planar.

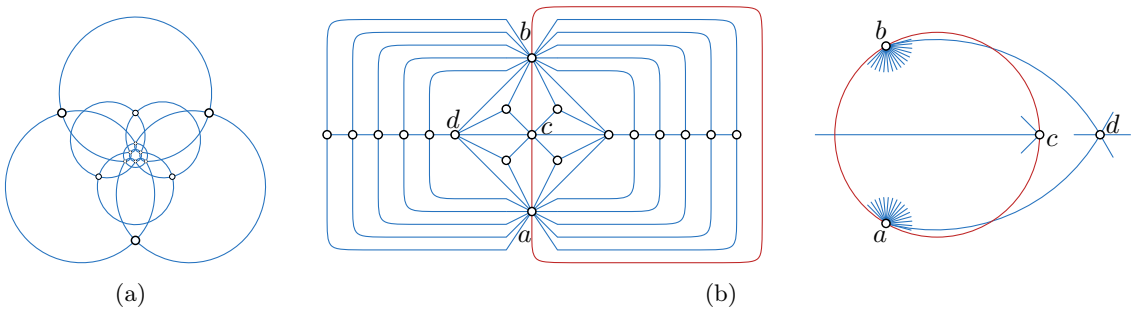

Figure 7: (a) Nested triangles graph with four levels that has no planar Lombardi drawing [15]. (b) Left: A planar 3-tree that has no planar Lombardi drawing. Right: For the K_4 subgraph defined by the four vertices a, b, c, and d, a drawing with the correct angles at each vertex must necessarily have crossings.

3.1 A Planar 3-tree with no Planar Lombardi Drawing

It is known that planar graphs do not necessarily have planar Lombardi drawings. For example, Duncan et al. [15] show that the nested triangles graph must have edge crossings whenever there are 4 or more levels of nesting, see Figure 7(a). While this graph is 4-degenerate, even more constrained classes of planar graphs have no planar Lombardi drawings. Specifically, we can show that there exists a planar 3-tree that has no 1-Lombardi planar realization. The planar 3-trees, also known as Apollonian networks and stacked triangulations, are the planar graphs that can be formed, starting from a triangle, by repeatedly adding a vertex within a triangular face, connected to the three triangle vertices, subdividing the face into three smaller triangles. These graphs have attracted much attention within the physics research community both as models of porous media with heterogeneous particle sizes, and as models of social networks [3]. In addition, 3-trees are relevant for Lombardi drawings because they are examples of 3-degenerate graphs, which have nonplanar Lombardi drawings if vertex-vertex and vertex-edge overlaps are allowed.

An example of a planar 3-tree that has no planar Lombardi drawing is given in Figure 7(b); in the figure, there sixteen vertices other than a, b and c, but our construction

requires a sufficient number (which we do not specify precisely) in order to force the angle between arcs $\widehat{ad}$ and $\widehat{ab}$ to be arbitrarily close to 180°. The numbers of vertices on the top and bottom of the figure should be equal. Because of this equality, the three arcs $\widehat{ab}$, $\widehat{bc}$, and $\widehat{ca}$ split the graph into two isomorphic subgraphs, and due to this symmetry they must meet at 180° angles to each other, necessarily forming a circle in any Lombardi drawing. By performing a Möbius transformation[1] on the drawing, we may assume without loss of generality that these three points form the vertices of an equilateral triangle inscribed within the circle, as shown in the right of the figure. Then, according to the previous analysis of 3-degenerate Lombardi graph drawing [15], there is a unique point in the plane at which vertex d may be located so that the arcs $\widehat{ad}$, $\widehat{bd}$, and $\widehat{cd}$ form the correct 120° angles to each other and the correct angles to the three previous arcs $\widehat{ab}$, $\widehat{bc}$, and $\widehat{ca}$. However, as shown on the right of the figure, that unique point lies outside circle abc and causes multiple edge crossings in the drawing.

3.2 Outerpaths

We define an *outerpath* to be a triangulation (we later lift this restriction) of the convex hull of a set of points on two parallel lines, or equivalently to be a triangulated outerplanar graph whose weak dual (the adjacency graph of the triangular faces) is a path. Like all outerplanar graphs, outerpaths have treewidth at most two. As we now show, every outerpath is Lombardi.

The idea is to look at the ordered dual of the given outerpath G, which keeps track of left and right turns made by the dual path. Each group of consecutive turns of the same type defines a fan of triangles. We can draw the path with straight-line segments so that each k-fan corresponds to a nearly complete drawing of a regular k-gon. These k-gons are stitched together by edges whose duals correspond to edges in adjacent fans.

We define the *spine* of G to be the path connecting all vertices of degree greater than 3. We root the spine at one of its endpoints, v_1, and denote the remaining spine vertices as $v_2, \ldots, v_s$ along the rooted path. We define the *hull* of G to be the cycle bounding the outer face. Finally, we define the *petals* of G to be the remaining edges, grouped into connected components called *flowers*. Figure 8 shows an example.

Applying Property 2 along the dual path of G and drawing all petals with straight edges fixes the whole structure of each flower (up to rigid transformations and scaling), with one remaining degree of freedom in the connection of each pair of flowers. In Figure 8(b), we used the remaining degree of freedom to fix all spine edges to be straight-line edges as well, leading to a nice drawing. Such drawings, however, are not necessarily planar. We note that once one flower is drawn, the allowed locations of the next spine vertex lie on a circle by Property 2, which determines the scale of the next flower.

For a vertex v of G, we write χ_v to denote its degree. For a spine vertex v_i we say that it is an *upward* (*downward*) vertex if in counterclockwise order of its neighbors v_{i-1} is the predecessor (successor) of v_{i+1}. Note that along the spine, upward and downward

[1] A Möbius transformation [5] is a transformation of the plane, which maps circles to circles and preserves angles. Hence a Lombardi drawing is transformed into another Lombardi drawing.

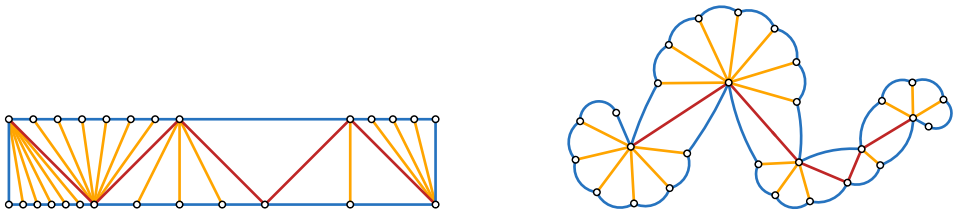

(a) (b)

Figure 8: (a) An outerpath. (b) A Lombardi drawing of the outerpath. The *spine* consists of the red edges, the *hull* consists of the blue edges, *petals* are yellow, and connected components of petals form *flowers*.

vertices alternate. For every vertex v we define its (spine/hull/petal) *stubs* as the χ_v equally spaced tangent vectors that describe the orientations of all incident (spine/hull/petal) edges of v.

The next lemma classifies the problematic quadrilaterals that can appear in outerpaths. Let $\alpha, \beta, \gamma, \delta$ be the four inner angles of a quadrilateral and let $\sigma = \alpha + \gamma - \beta - \delta$ as in Section 2. There are two types of quadrilaterals in outerpaths that are characterized as follows.

Lemma 1. *Let P be an outerpath with n vertices. Every arc quadrilateral formed by two adjacent triangles of P has $\sigma < 360°$ in a planar Lombardi drawing of P, unless it is formed by one hull vertex and three consecutive spine vertices a, b, and c with $\chi_b = 5$ and $1/\chi_a + 1/\chi_c \leq 1/15$.*

Proof. Let $\diamondsuit abcd$ be a quadrilateral with $\sigma \geq 360°$ that is part of a planar Lombardi drawing of P. Note that two of the opposite angles involved are formed by neighboring edges and thus are *Lombardi angles* (they are $360°/\chi_v$ for some vertex v), and the other two are *double Lombardi angles* (they are $720°/\chi_v$ for some vertex v) as they span over the diagonal of $\diamondsuit abcd$. Lombardi angles are at most $120°$, so the two Lombardi angles cannot sum to more than $240° < 360°$. So, assume w.l.o.g. that α and γ are the double Lombardi angles and that $\alpha + \gamma - \beta - \delta \geq 360°$. Now, $\alpha + \gamma > 360°$, since no angles are $0°$, so at least one of α or γ needs to be larger than $180°$. In fact, this means one of them must be $240°$, say $\alpha = 240°$, and $\chi_a = 3$. This further implies that the two triangular faces of the quadrilateral are incident to two adjacent hull edges. Now, $\chi_c > 3$ (unless there are only four vertices in G), so $\gamma \leq 180°$. If either b or d has degree 3, then β or δ is $120°$, which means that $\alpha + \gamma - \beta - \delta$ would be smaller than $360°$. Therefore, b, c, and d are all vertices of degree greater than 3, i.e., they are part of the spine. This implies $\chi_c = 5$ (there is only one petal edge between the two spine edges, and then there are two hull edges), so $\gamma = 144°$. This means $\beta + \delta \leq 240° + 144° - 360° = 24°$. That is, the degrees of b and d are such that $1/\chi_b + 1/\chi_d \leq 1/15$. □

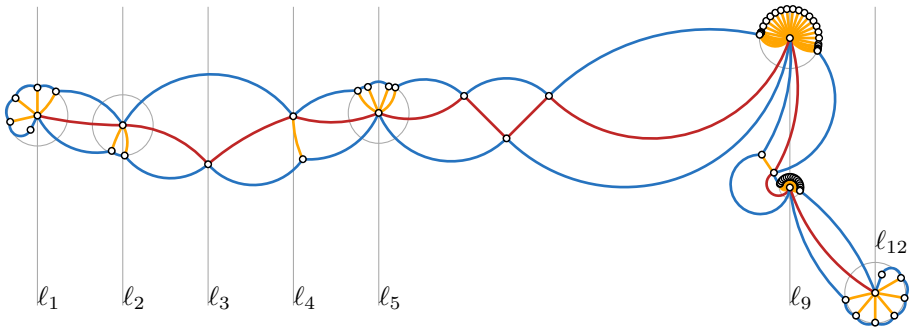

Figure 9: A Lombardi drawing of an outerpath with spine degrees 7, 6, 4, 5, 8, 4, 4, 4, 30, 5, 30, and 9, which exhibits the different cases considered by our algorithm (we did cheat a little in that we used a larger value for ε for all vertices except v_{11}, for better visibility).

3.2.1 Algorithm for Planar Drawing of Outerpaths

The main idea for drawing an outerpath in Lombardi style is to draw the spine in an x-monotone fashion, and draw the petals in sufficiently small circles around the spine vertices so that they do not intersect each other. To this end, we align every spine vertex so that both of its spine stubs leave it at opposite angles with respect to a vertical line. This method works well as long as all spine vertices have sufficiently high degree; however, we need to abort this general scheme in several cases involving spine vertices of degree 4 or 5.

Our algorithm to draw outerpaths proceeds in two main phases. In the first phase, we draw the spine and all hull edges connecting two spine vertices. In the second phase we draw the flowers for each spine vertex by incrementally adding the petals. Figure 9 shows an example output as produced by the algorithm.

Spine. Let the spine vertices be $v_1, \ldots, v_s$ as they occur along the spine. We initially put vertex v_1 at the origin $(0, 0)$ and rotate it so that the vertical line $\ell_1 : x = 0$ bisects the angle between the tangents of its two incident hull edges. In all subsequent steps, the placement of the next vertex v_i depends on its degree χ_{v_i} and the degrees of its neighbors. In the general case $\chi_{v_i} > 5$ we place v_i on the vertical line ℓ_i at distance 1 from v_{i-1} at the unique position where a circular arc from v_{i-1} tangent to the outgoing spine stub of v_{i-1} intersects ℓ_i at an angle of $\pm 1.5 \cdot 360°/\chi_{v_i}$ depending on whether v_i is an upward or downward spine vertex. We draw the circular arc that defined the position of v_i as the spine edge from v_{i-1} to v_i; see Figure 9. The same procedure still applies if $\chi_{v_i} = 5$ and $1/\chi_{v_{i-1}} + 1/\chi_{v_{i+1}} > 1/15$.

If $\chi_{v_i} = 5$ and $1/\chi_{v_{i-1}} + 1/\chi_{v_{i+1}} \leq 1/15$, we switch from a horizontal placement mode to a vertical one, see Figure 10. This is necessary to avoid edge crossings according to Lemma 1. The first step is to modify v_{i-1} by rotating it so that the spine stub towards v_i is left of ℓ_{i-1} by 12°. We skip v_i for the moment and place v_{i+1} vertically above or below v_{i-1}, depending on whether v_{i-1} is a downward or upward vertex, and so that its hull stub towards v_{i+2} is vertical. If v_{i+1} is placed below v_{i-1}, the position is chosen such that there is a vertical distance of 1 to the lower of v_{i-1} and v_{i-2}; we choose the analogous position if it is placed above v_{i-1}. Now that both v_{i-1} and v_{i+1} are placed, we construct the placement

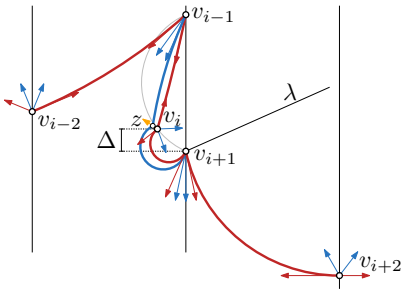

Figure 10: Vertical placement of a degree-5 vertex v_i with two high-degree neighbors.

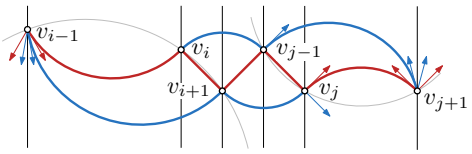

Figure 11: Placement of a chain of degree-4 spine vertices $v_i, \ldots, v_j$.

circle C for v_i based on its two spine neighbors and the angle $\theta_{v_{i-1}v_{i+1}} = 3 \cdot 72° = 216°$, see Figure 10. We choose a position for v_i on C that has a small vertical distance Δ from v_{i+1} (see Lemma 3) and connect it with two arcs to its spine neighbors. Note that this vertical structure repeats if another degree-5 vertex with the same properties follows; otherwise we continue by placing v_{i+2} horizontally to the right on a vertical line ℓ_{i+2} that has the same distance to v_{i+1} as the distance between the first and third vertex of the vertical structure.

If $\chi_{v_i} = 4$ and $\chi_{v_{i+1}} > 4$, we make an exception and first draw v_{i+1}, and the hull edge connecting it to v_{i-1} in this case. Vertex v_{i+1} is placed on the vertical line ℓ_{i+1} at distance 2 from v_{i-1}. The position is the unique intersection point of ℓ_{i+1} and the circular arc from v_{i-1} tangent to the outgoing hull stub of v_{i-1}, where the angle between the arc and ℓ_{i+1} is $\pm 0.5 \cdot 360°/\chi_{v_{i+1}}$ depending on whether v_{i+1} is upward or downward. Now that v_{i-1} and v_{i+1} are both placed, we put v_i at the intersection point of the vertical line ℓ_i centered between ℓ_{i-1} and ℓ_{i+1} and the placement circle of v_i with respect to v_{i-1}, v_{i+1} and an enclosed angle of $\theta_{v_{i-1}v_{i+1}} = 90°$ according to Property 2. See vertex v_3 on line ℓ_3 in Figure 9 for an example.

Finally, if $\chi_{v_i} = \cdots = \chi_{v_j} = 4$ $(i < j)$ for a maximal sequence of $j + 1 - i$ vertices, we place the whole sequence at once, see Figure 11. Both the spine edge from v_{i-1} to v_i and the hull edge from v_{i-1} to v_{i+1} should intersect the vertical lines ℓ_i and ℓ_{i+1} at an angle of $\pm 45°$. In order to achieve this, we place ℓ_i at distance 1 from v_{i-1} and find the position of v_i as done before. Since v_{i+1} is connected by a spine edge to v_i and by a hull edge to v_{i-1} this defines a placement circle for v_{i+1} and we pick the unique position for which the edge v_iv_{i+1} is straight, see Figure 11. Now we can draw the whole chain of degree-4 vertices in a zigzag fashion using the horizontal spacing defined by ℓ_i and ℓ_{i+1}. For the vertex v_{j+1} with $\chi_{v_{j+1}} > 4$ we construct the placement circle with respect to v_{j-1}, v_j, and the angle $\theta_{v_{j-1}v_j} = 360°/\chi_{v_{j+1}}$ and choose the position for which the angle between the vertical line ℓ_{j+1} and the arc $\overset{\frown}{v_jv_{j+1}}$ is $\pm 1.5 \cdot 360°/\chi_{v_{j+1}}$.

Lemma 2. *The spine does not intersect itself.*

Proof. Recall that if v_i and v_{i+1} are two vertices of degree not 5, then they are placed on vertical lines ℓ_i and ℓ_{i+1}. Since the spine stub of v_i points to the right and that of v_{i+1} points to the left, the spine edge stays within this vertical strip and no two spine edges intersect.

Now, let v_i be a vertex with $\chi_{v_i} = 5$ and its spine neighbors with $1/\chi_{v_{i-1}} + 1/\chi_{v_{i+1}} \leq 1/15$; they are placed on a common vertical line ℓ. Assume w.l.o.g. that v_{i-1} and v_{i+1} are upward vertices as in Figure 10. Then both arcs $\widehat{v_{i-1}v_i}$ and $\widehat{v_iv_{i+1}}$ lie completely to the left of ℓ. On the left of ℓ, $\widehat{v_{i-2}v_{i-1}}$ and $\widehat{v_iv_{i+1}}$ could intersect, but since the left spine stub of v_{i-1} has a nonzero slope, there is a placement of v_i on its placement circle where $\widehat{v_iv_{i+1}}$ lies completely to the right of the line supported by this stub. □

Flowers. Let $\varepsilon' > 0$ be a number such that we can place a disk of radius ε' around every spine vertex such that it does not intersect any spine edges other than those incident to the vertex, and such that no two such disks intersect. Lemma 2 implies this number exists. To compute a suitable value for ε', we check for each spine vertex which spine edge is closest to it; because of the monotone structure in our construction there are only constantly many candidates so this takes $O(n)$ time in total. Now, for each spine vertex of degree at least 6, we preliminarily place the two outermost petal vertices at the intersection of their placement circles and these disks of radius ε'.[2] The hull edges connecting them to their neighboring spine vertices together with any hull edges that are incident to at least one spine vertex are called the *preliminary hull*.

Lemma 3. *The preliminary hull edges do not have intersections with each other or the spine.*

Proof. The proof of this lemma is similar to that of Lemma 2, but some extra care needs to be taken. First, let v_i and v_{i+1} be two vertices of degree at least 6. Then the hull edges connecting v_i to the first petal vertex of v_{i+1} and connecting v_{i+1} to the last petal vertex of v_i still lie completely in the vertical strip between ℓ_i and ℓ_{i+1}.

Chains of multiple vertices of degree 4 are still vertically aligned, so the same argument applies. Now, let v_i be a degree 4 vertex with spine neighbors of degree at least 5. Then v_i could be drawn slanted. However, then $\widehat{v_{i-1}v_{i+1}}$ is the only hull edge on one side of the spine inside the vertical strip between ℓ_{i-1} and ℓ_{i+1}, and the two hull edges on the other side that connect v_i to the petal vertices of v_{i-1} and v_{i+1} are adjacent and also lie within this strip. So, they do not intersect each other either.

Finally, consider again the vertical case where v_i is a degree-5 vertex with spine neighbors whose degrees satisfy $1/\chi_{v_{i-1}} + 1/\chi_{v_{i+1}} \leq 1/15$ as in Figure 10. Let z be the single petal vertex of v_i. On the left, we first need to argue that $\widehat{zv_{i-1}}$ does not intersect any other arc. Obviously, it runs below the arc from v_{i-1} to the last petal of v_{i-2} until the height of v_{i-2}; thereafter it has either already reached its leftmost point and goes right towards v_i or is short enough to not reach too far left anyway. Secondly, we need to argue that $\widehat{zv_{i+1}}$ does not intersect the leftward hull edge emanating from v_{i-1}; as before we can ensure this by moving the location of v_i (and therefore, also z) sufficiently close to v_{i+1}; this vertical distance is denoted Δ in the algorithm. On the right, we need to argue that the hull edge emanating from v_i toward the flower of v_{i-1} does not intersect the leftward hull edge emanating from v_{i+2}. Since $1/\chi_{v_{i-1}} + 1/\chi_{v_{i+1}} \leq 1/15$ we know that $\chi_{v_{i+1}} \geq 15$ and hence the angle between two neighboring stubs of v_{i+1} is at least 24°. Now, let λ be the

[2] Note that for a spine vertex of degree 5 there is a unique position for placing its only petal vertex.

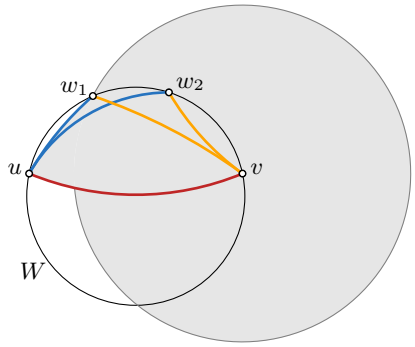

Figure 12: Illustration for the proof of Lemma 4

line through v_{i+1} that makes an angle of 114° with ℓ_{i-1}. If v_i is sufficiently close to v_{i+1}, its hull stub forms an angle of less than 66° with ℓ_{i-1}, so its hull edge lies completely above λ. The angle at which the spine arc $\widehat{v_{i+1}v_{i+2}}$ meets ℓ_{i-1} is at most 24°; since $\chi_{v_{i+2}} \geq 4$ this means that the angle at which the hull edge towards the flower of v_{i+1} comes in is at most $90° + 24° = 114°$. Hence, this hull edge lies below λ, and the two hull edges in the strip between $\ell_{v_{i-1}}$ and $\ell_{v_{i+2}}$ do not intersect. □

By Lemma 3, the preliminary hull does not intersect itself or the spine, but it could still intersect some of the ε'-disks. Therefore, we now compute a new value $\varepsilon < \varepsilon'$ such that disks of radius ε placed at the spine vertices do not intersect any spine or hull edges. We will draw the flowers inside these ε-disks; Lemma 4 implies that the resulting drawing of the hull edges will still be planar after shrinking the disks to radius ε.

Lemma 4. *Let u, v be two adjacent spine vertices and w the first petal vertex of v (this implies that w is connected to u by a hull edge). Let w_1 and w_2 be two possible locations for w on its placement circle W through u and v, such that w_1 lies closer to u and w_2 lies closer to v. Then the hull edge connecting u to w_2 lies completely inside the region bounded by $\widehat{uv}$, $\widehat{uw_1}$, and the circle centered at v of radius $|vw_1|$.*

Proof. Consider the circle W of possible placements for w as shown in Figure 12. Both w_1 and w_2 lie on W. The edges $\widehat{uw_1}$ and $\widehat{uw_2}$ both leave u in the same direction and with the same tangent. Hence, they are arcs of two touching circles, which do not intersect other than at u. Furthermore, since w_1 is closer to u, the edge $\widehat{uw_2}$ lies completely inside the region bounded by $\widehat{uv}$, $\widehat{uw_1}$, and the circle centered at v of radius $|vw_1|$ as claimed in the lemma statement. □

We now describe how to draw the actual flowers recursively. Let C be a circle centered at a spine vertex v; let u and w be two points on C and let $\widehat{uv}$ and $\widehat{vw}$ be two arcs that lie completely inside C and have nonnegative curvature, and let $\nu \geq 0$ be an integer. We will create ν stubs at v, equally spaced between $\widehat{vu}$ and $\widehat{vw}$, and draw $\nu+2$ petal vertices (including u and w, which could be moved).

If $\nu \geq 2$, we keep both u and w where they are, and we proceed by drawing a circle D slightly smaller than C (say, of radius $\frac{n-1}{n}$ times smaller). By Property 2, there is a

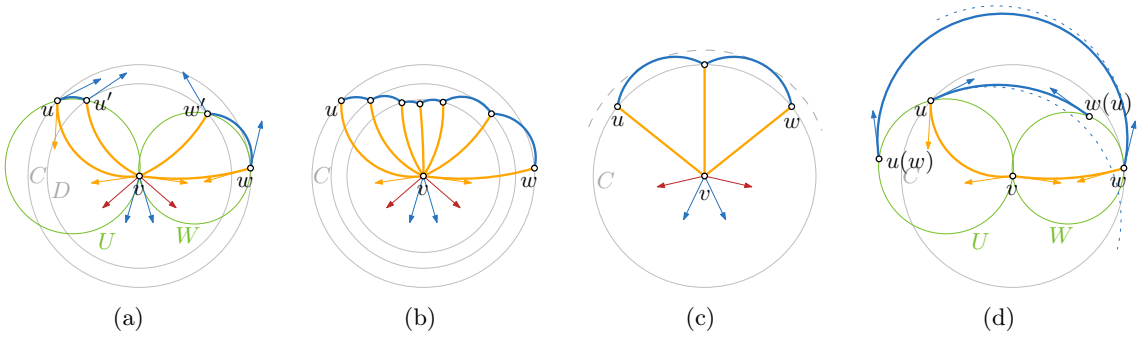

Figure 13: (a) A partially drawn flower. (b) A possible completion of the flower. (c) In the worst case, the petals do not protrude more than a factor 1.2 out of C. (d) If Lombardi edges from u and w do not match up, then one of them overshoots the other and the other one undershoots the first (dotted).

circle U of possible placements of the petal vertex u' adjacent to u, that connects to v at the next stub and makes an angle of 120° at u'. Symmetrically, there is a circle W of possible placements of the petal vertex w' adjacent to w. We intersect U and W with D, and place u' and v' at the intersection points to the right (resp. to the left) of $\widehat{uv}$ (resp. $\widehat{vw}$). Figure 13(a) illustrates this. Now, we recurse on the smaller problem defined by D, u', and w'.

If $\nu = 1$, we simply compute the circles U and W and place the last vertex x at one of the intersection points of U and W. One of the two intersection points is v; we place x at the other one.

Finally, if $\nu = 0$, we cannot generally place u and w at their given location. Instead, either we fix u and place $w(u)$ at the intersection between the two placement circles based on where u is, or we fix w and place $u(w)$ at the intersection between the two placement circles. If we fix u and $w(u)$ is closer to v than w, we are done. Otherwise, it must be the case that if we fix w then $u(w)$ is closer to v than u is, and we are also done. To see this, draw an arc that leaves u at the correct angle until it has the angle at which it should enter w, and vice versa; if one of these "overshoots" its target the other must "undershoot" it (refer to Figure 13(d)).

We apply the above algorithm to each spine vertex, choosing C to be the circle centered at v of radius $\frac{5}{6}\varepsilon$, and choosing u and w to be the two petal vertices we get at the intersection of C with their respective placement circles. As soon as we fix any petal vertex, we can immediately draw the hull edge connecting it to the previously fixed petal neighbor (or the spine neighbor in case of the two outermost petals).

The only remaining case is to draw a flower with exactly one petal. Let v_i be the spine vertex and w the adjacent petal vertex. In this case we know that w connects to v_{i-1} and to v_{i+1} by two hull edges. We can simply intersect the two placement circles for w and and meeting angle of 120°, one with respect to v_{i-1} and v_i, the other with respect to v_i and v_{i+1}. One intersection point is v_i, at the other one we place w and draw its three incident edges. This concludes the second phase of the algorithm.

Lemma 5. *The flower algorithm produces an internally planar drawing that is contained within a circle of radius at most* 1.2 *times bigger than* C.

Proof. For the first part of the lemma, we need to show that each time we place a petal vertex, it lies on the correct side of the previous petal edge. In the $\nu \geq 2$ case, we note that D separates v from u and w, U passes through v and u, and W passes through v and w, so D intersects both U and W. Since the curvature of $\widehat{uv}$ is nonnegative, there must be at least one intersection point of D and U to the right of this arc; similarly since $\widehat{vw}$ is non-negative there must be at least one intersection point of D and W to the left of this arc. If the radius of D is sufficiently close to that of C, the ordering is correct (i.e. u' lies to the left of w').

In the $\nu = 1$ case, we need to use the fact that this is the last point to be placed, so the angle between $\widehat{uv}$ and $\widehat{vw}$ at v is at most $2 \cdot 360°/7$. Since the angle at x is 240°, and $240 + \frac{2}{7}360 < 360$, we clearly have $\sigma < 360°$. When $\chi_{v_i} = 5$ or 6, planarity is clear since there are only one or two petal vertices; if $\chi_{v_i} = 5$, this clearly relies on $1/\chi_{v_{i-1}} + 1/\chi_{v_{i+1}}$ being greater than $1/15$.

Finally, we argue that this construction stays inside a circle C' of radius at most 1.2 times larger than C. We only need to consider the arcs incident to u and w; then the rest follow again by induction. Now, note that the amount of protrusion of the hull edges between petal vertices depends on the outgoing angle at u (or w), as well as the distance to the next vertex. The outgoing angle is 30° in the worst case, because the curvature of $\widehat{uv}$ is nonnegative. The distance to the next vertex is $360°/6$ in the worst case, because $\chi_v \geq 6$. The claim now follows from basic goniometry. Figure 13(c) shows an example. □

Once we have placed the spine and all flowers as described above, it is clear that by construction the resulting drawing satisfies the Lombardi properties, i.e., circular-arc edges and perfect angular resolution. The previous lemmas prove that the drawing produced by our algorithm is indeed planar. Since every vertex is placed by computing local information only, the algorithm takes linear time. We summarize the result.

Theorem 1. *Every outerpath has an outerplanar Lombardi drawing that can be constructed in linear time.*

Non-Triangulated Outerpaths The algorithm we presented assumes the input outerpath is triangulated. This is not a restriction, as the next corollary shows.

Corollary 1. *Given an algorithm to draw triangulated outerpaths, we can draw any outerpath.*

Proof. For a face of size four or more we distinguish two cases. It is clear that in an outerpath there can be at most two non-hull edges in each face. If all hull edges form one connected path in the face, then we can replace this path by a single hull edge to get a triangular face and re-insert the degree-2 vertices in the end. Since that subdivides a circular arc, all angles are 180° as necessary.

If the hull edges form two disconnected paths, we temporarily remove all degree-2 vertices on the two hull paths as before. This yields a quadrilateral face f that interrupts the spine and is bounded by two hull edges and two petals. Next, we introduce a diagonal dummy spine edge $e = uv$ that connects the left vertex u of one hull edge with the right vertex v of the other hull edge. To get the Lombardi angles right in the end, we make sure that the dummy edge does not count towards the vertex degrees χ_u and χ_v and hence does not affect the prescribed angles around the two vertices. The only exception is that the four angles defined by uv and the four edges of f are set to $1/2 \cdot 360°/\chi_u$ and $1/2 \cdot 360°/\chi_v$, respectively, i.e., each dummy edge bisects the two Lombardi angles on either endpoint. Hence, the drawing obtained by removing all dummy edges and re-inserting all omitted degree-2 vertices is a planar Lombardi drawing of the given outerpath. □

4 k-Lombardi Drawings

In this section, we investigate k-Lombardi drawings. First, we establish the need to use poly-arc edges in order to be able to draw any graph.

4.1 Non-Lombardi Graphs

Duncan et al. [15] show a graph, Figure 14(a), for which no Lombardi drawing is possible *while preserving the given ordering of edges around each vertex*. However, as Figure 14(b) shows, if the ordering is not fixed, it is possible to create a valid Lombardi drawing for the graph. In this section, we provide a graph that has no Lombardi drawing *regardless of the edge ordering*.

There are some complications that arise when proving that a graph is non-Lombardi, compared to proving that a graph is not part of a graph class in traditional straight-line planar drawings. For example, if graph G is non-Lombardi, this does not imply that all graphs $H \supset G$ are non-Lombardi because the addition of edges changes the angular resolution and can therefore dramatically change the subsequent placement of vertices. In addition, since the edge ordering is not fixed by the input, we must argue that any ordering forces a conflict.

Additional complications concern the density and symmetry of any possible counterexample. The graph in Figure 14 is 3-degenerate, and 3-degenerate graphs can be drawn Lombardi-style if we are willing to ignore vertex-vertex and vertex-edge overlaps [15] (as shown in Figure 14(a)). Consequently, if a 3-degenerate graph is to be a counterexample, we must show that all vertex orderings force at least two vertices to overlap. Intuitively, 4-degenerate graphs should be more restrictive, but the simplest 4-degenerate graph, K_5, nevertheless has a circular Lombardi drawing. One issue is the fact that K_5 is extremely symmetrical. Therefore, we shall modify this graph to break its symmetry. We define our counterexample graph G_8 to be K_5 with the addition of three degree-one vertices causing one of the vertices of the original K_5 to have degree 5 and another to have degree 6, while the other three remain with degree 4; see Figure 15(a).

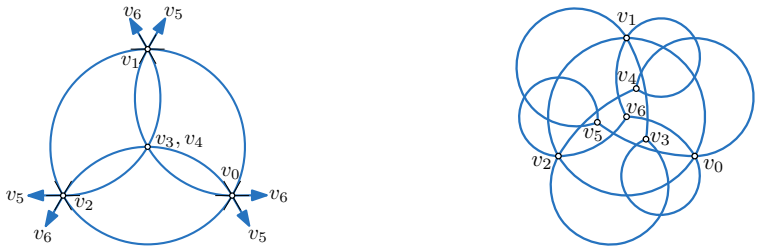

(a) (b)

Figure 14: A 7-vertex 3-degenerate graph that has no Lombardi drawing with the given edge ordering. (a) A Möbius transformation makes one triangle equilateral, forcing the other 4 vertices to be placed at the centroid and the point at infinity; (b) A different ordering that does provide a Lombardi drawing.

(a) (b)

Figure 15: (a) G_8 with K_5 part drawn Lombardi-style and additional edges shown. (b) Computing the twist for the three vertices 0, 1, and 2. The twist for vertex 0 is ξ.

4.1.1 Proof of Non-Lombardiness

Theorem 2. *The graph G_8 is non-Lombardi.*

Proof. Let v_0, v_1, v_2 be the three vertices of G_8 with degree four. Let v_3 and v_4 be the vertices with degree five and six, respectively. We do not care about the final placement of the degree-one vertices, whose main purpose is to alter the angular resolution of v_3 and v_4. Using a Möbius transformation we can assume that the first three vertices v_0, v_1, and v_2 are placed on the corners of a unit equilateral triangle such that v_0 and v_1 have positions $(0, 0)$ and $(1, 0)$ respectively. We shall show that for every edge ordering, the two vertices v_3 and v_4 cannot both be placed to maintain correctly their angular resolution and be connected to each other. We do this by establishing the algebraic equations for their positions based on the edge orderings of all vertices. We then show that such a set of equations has no solution for any valid assignment of orderings.

We first establish a notation for representing a specific edge ordering. For every vertex v_i with neighbor v_j, let k_{ij} represent the cyclic ordering of edge (v_i, v_j) about v_i with $k_{01} = 0$ and $k_{i0} = 0$ for $i > 0$. For example, in Figure 15(a), the edge ordering around v_4 has $k_{41} = 2$, $k_{42} = 4$, $k_{43} = 5$, $k_{46} = 1$, and $k_{47} = 3$. The *twist* φ_i of a vertex v_i is the angle made by the arc extending from v_i to the neighbor v_j with $k_{ij} = 0$. From

the initial placement of v_0, v_1, and v_2 on an equilateral triangle and their respective edge orderings, we can uniquely determine the twists for each of these vertices; see Figure 15(b). Since the three vertices lie on an equilateral triangle, the tangents to the circle defined by the three points also form an equilateral triangle. From Property 1, the angles formed by the arcs connecting each pair of vertices to the tangents at the circle yield matching (but undetermined) angles, labeled ψ_a, ψ_c, and ψ_e. The angles ψ_b, ψ_d, and ψ_f are determined uniquely by the edge orderings as follows:

$$\psi_b = 2\pi - k_{02}\pi/2 \tag{1}$$
$$\psi_d = k_{12}\pi/2 \tag{2}$$
$$\psi_f = 2\pi - k_{21}\pi/2 \tag{3}$$

Noting that certain triplets of angles yield a value of π modulo 2π, we have the following three equations with $i_0, i_1, i_2 \in \{0, 1\}$:

$$\psi_a + \psi_b + \psi_c = \pi + 2i_0\pi \tag{4}$$
$$\psi_c + \psi_d + \psi_e = \pi + 2i_1\pi \tag{5}$$
$$\psi_e + \psi_f + \psi_a = \pi + 2i_2\pi. \tag{6}$$

Solving for ψ_a yields:

$$\begin{aligned}(\psi_a + \psi_b + \psi_c) - (\psi_c + \psi_d + \psi_e) + (\psi_e + \psi_f + \psi_a) &= (\pi + 2i_0\pi) - (\pi + 2i_1\pi) + (\pi + 2i_2\pi)\\ 2\psi_a + \psi_b - \psi_d + \psi_f &= 2\pi + 2(i_0 - i_1 + i_2)\pi\\ 2\psi_a &= \pi - \psi_b + \psi_d - \psi_f + 2(i_0 - i_1 + i_2)\pi.\end{aligned} \tag{7}$$

For the twist for v_0, we wish to know the value of ξ, the angle for the arc from v_0 to v_1. Noting that $\xi = \psi_a + \psi_b + 2\pi/3 - 2i_0\pi$ and substituting in Equations (1-3) with Equations (7) yields

$$\begin{aligned}2\xi &= 2\psi_a + 2\psi_b + 4\pi/3 - 4i_0\pi\\ 2\xi &= (\pi - \psi_b + \psi_d - \psi_f + 2(i_0 - i_1 + i_2)\pi) + 2\psi_b + 4\pi/3 - 4i_0\pi\\ 2\xi &= 7\pi/3 + \psi_b + \psi_d - \psi_f + 2(i_2 - i_0 - i_1)\pi\\ 2\xi &= 7\pi/3 + (2\pi - k_{02}\pi/2) + (k_{12}\pi/2) - (2\pi - k_{21}\pi/2) + 2(i_2 - i_0 - i_1)\pi\\ 2\xi &= 7\pi/3 + (k_{12} + k_{21} - k_{02})\pi/2 + 2(i_2 - i_0 - i_1)\pi\\ \varphi_0 = \xi &= 7\pi/6 + (k_{12} + k_{21} - k_{02})\pi/4 + (i_2 - i_0 - i_1)\pi.\end{aligned} \tag{8}$$

Noting that $\varphi_0 + \psi_c + \pi/3 = 2\pi$ yields $\varphi_1 = \pi - \varphi_0$. Similarly, $\varphi_2 = \pi - \psi_a = 5\pi/3 - \varphi_0 - k_{02}\pi/2 + 2(1 - i_0)\pi$.

The positions and orienting twists of the first three vertices also yield a unique position and twist for vertices v_3 and v_4. After determining these values, we shall show that in all orderings it is not possible to connect v_3 to v_4 with a single circular arc while still maintaining the proper angular resolution.

From Property 2, v_3 must lie on a circle C_{01} defined by the neighbors v_0 and v_1 and their corresponding arc tangents. Similarly, it must lie on circles C_{02} and C_{12}. The

intersection of these three circles determines the position and orientation of v_3. Let us proceed to determine C_{01}. Letting $p = v_0$ and $q = v_1$, we have $\theta_{ph} = \varphi_0 + \pi k_{03}/4$ and $\theta_{qh} = \varphi_1 + \pi k_{13}/4$ and $\theta_{pq} = \pi(k_{31} - k_{30})/5 = \pi k_{31}/5$. From Property 2 and the fact that $d_{pq} = 1$, we can determine that C_{01} has radius $r_{01} = \csc\alpha_{01}/2$ and center $c_{01} = (r_{01}\sin\alpha_{01}, -r_{01}\cos\alpha_{01}) = (1/2, -\cot\alpha_{01}/2)$ with $\alpha_{01} = (\theta_{ph} - \theta_{qh} - \theta_{pq})/2 = \varphi_0 - \pi/2 + \pi(5k_{03} - 5k_{13} - 4k_{31})/40$. Similarly, C_{02} has radius $r_{02} = \csc\alpha_{02}/2$ and center $c_{02} = (r_{02}\sin(\alpha_{02} + \pi/3), -r_{02}\cos(\alpha_{02} + \pi/3)$ with $\alpha_{02} = \varphi_0 - 5\pi/6 + \pi(5k_{03} + 10k_{02} - 5k_{23} - 4k_{32})/40 + (i_0 - 1)\pi$.

Given the circles and the position of v_0 at the origin, it is easy to determine the intersection of the two circles, one of which is v_0 and the other, if it even exists, must be v_3. Since v_0 must lie on the intersection, the line from v_0 to v_3 is perpendicular to the line, ℓ, through the two centers. Moreover, v_3 is the reflection of p about ℓ. Thus, letting $\vec{v} = (v_x, v_y) = c_{02} - c_{01}$, $\vec{c} = v_0 - c_{01} = -c_{01}$, and $\vec{v}^{\perp} = (-v_y, v_x)$ yields

$$v_3 = \frac{-2\vec{c}\cdot\vec{v}^{\perp}}{\vec{v}\cdot\vec{v}}\vec{v}^{\perp}. \tag{9}$$

To establish the twist φ_3 at v_3 we observe from Property 1 that the angle α formed by the line ℓ_{03} from v_0 to v_3 and the tangent of the curve from v_0 to v_3 is the same as the tangent of the curve from v_3 to v_0 and the line ℓ_{03}. Moreover, $\theta_{03} = \varphi_0 + k_{03}\pi/4 = \alpha + \beta_{03}$ and $\varphi_3 = \theta_{30} = \pi - \alpha + \beta_{03}$ where $\beta_{03} = \arctan(v_3(y)/v_3(x))$ is the slope of ℓ_{03}. From this, we can deduce that $\varphi_3 = \pi - \varphi_0 - k_{03}\pi/4 + 2\beta_{03}$. The exact same calculations can be used to compute v_4 and φ_4.

As with the twists for φ_3 and φ_4, we can use Property 1 to determine the angles formed by the arc from v_3 to v_4 given their positions and twists. We know that the angles of the tangents to the arc at v_3 and v_4 are $\theta_{34} = \varphi_3 + k_{34}\pi/5$ and $\theta_{43} = \varphi_4 + k_{43}\pi/6$ respectively. Letting $\beta_{34} = \arctan((v_4(y) - v_3(y))/(v_4(x) - v_3(x)))$ be the slope of the line from v_3 to v_4, we have that $\theta_{34} - \beta_{34} = \alpha$ and $\pi - \alpha = \theta_{43} - \beta_{34}$. Consequently, we have

$$\theta_{34} + \theta_{43} = \pi + 2\beta_{34}. \tag{10}$$

Each specific edge ordering therefore yields a unique set of positions and twists for v_3 and v_4 as outlined above. To show that no Lombardi drawing is possible one must simply show that Equation 10 does not hold for *any* edge ordering. Though there are a finite number of possible orderings and though symmetries could be used to reduce that number, the individual case analysis for such a proof appears to be quite unwieldy. Instead, we simply iterate over every possible edge ordering, applying these equations to a numerical algorithm that searches for a valid non-contradictory assignment. The Python code for this program is shown in Table 1. As can be seen from the code, it verifies using floating-point calculations with 100-bit precision that each edge ordering has angles that are farther than $\epsilon = 10^{-6}$ from satisfying Equation 10. By running this program, one can see that no valid assignments are possible concluding our proof. □

Corollary 2. *There are an infinite number of biconnected non-Lombardi graphs.*

```
#!/usr/bin/python

from itertools import *
from bigfloat import *

def match(k0,k1,k2,k3,k4,i0,i1,i2):
    (k01,k02,k03,k04)=(0,k0[0],k0[1],k0[2])
    (k10,k12,k13,k14)=(0,k1[0],k1[1],k1[2])
    (k20,k21,k23,k24)=(0,k2[0],k2[1],k2[2])
    (k30,k31,k32,k34)=(0,k3[0],k3[1],k3[2])
    (k40,k41,k42,k43)=(0,k4[0],k4[1],k4[2])
    b,d,f = 2 - k02/2.0, k12/2.0, 2-k21/2.0            # Eqs 1-3
    t0 = 7.0/6.0 + (k12 + k21 - k02)/4.0 + (i2-i0-i1)  # The twists

    # Compute v3 and t3
    a01 = t0 - 0.5 + (5*k03 - 5*k13 - 4*k31)/40.0
    a02 = t0 + i0-11.0/6.0 + (5*k03 + 10*k02 - 5*k23 - 4*k32)/40.0
    r01, r02 = 0.5/sin(a01 * const_pi()), 0.5/sin(a02 * const_pi())
    c01 = (0.5, -0.5/tan(a01*const_pi()))
    c02 = (r02*sin((a02 + 1.0/3.0)*const_pi()), -r02*cos((a02 + 1.0/3.0)*const_pi()))
    v = (c02[0] - c01[0], c02[1] - c01[1])
    M = 2.0 * (c01[1] * v[0] - c01[0] * v[1])/(v[0]*v[0]+v[1]*v[1])
    v3 = (-v[1] * M, v[0] * M)
    b03 = atan2(v3[1], v3[0])/const_pi()
    t3 = 1 - t0 - k03/4.0 + 2*b03

    # Compute v4 and t4
    a01 = t0 - 0.5 + (3*k04 - 3*k14 - 2*k41)/24.0
    a02 = t0 + i0-11.0/6.0 + (3*k04 + 6*k02 - 3*k24 - 2*k42)/24.0
    r01, r02 = 0.5/sin(a01 * const_pi()), 0.5/sin(a02 * const_pi())
    c01 = (0.5, -0.5/tan(a01*const_pi()))
    c02 = (r02*sin((a02 + 1.0/3.0)*const_pi()), -r02*cos((a02 + 1.0/3.0)*const_pi()))
    v = (c02[0] - c01[0], c02[1] - c01[1])
    M = 2.0 * (c01[1] * v[0] - c01[0] * v[1])/(v[0]*v[0]+v[1]*v[1])
    v4 = (-v[1] * M, v[0] * M)
    b04 = atan2(v4[1], v4[0])/const_pi()
    t4 = 1 - t0 - k04/4.0 + 2*b04

    # Compare v3,t3 and v4,t4
    t34,t43 = t3 + k34/5.0, t4 + k43/6.0
    b34 = atan2(v4[1]-v3[1], v4[0]-v3[0])/const_pi()

    # Compare and account for small errors in round-off
    lhs, rhs = (t34 + t43, 1 + 2 * b34)
    diff = mod((lhs - rhs) if lhs > rhs else (rhs - lhs), 2)
    epsilon = 0.000001
    if (diff < epsilon or diff > 2-epsilon):
        return True    # Found a valid assignment

for k0 in permutations(range(1,4)):
    for k1 in permutations(range(1,4)):
        for k2 in permutations(range(1,4)):
            for k3 in permutations(range(1,5),r=3):
                for k4 in permutations(range(1,6),r=3):
                    for (i0,i1,i2) in product(range(0,2), repeat=3):
                        with precision(100):
                            if match(k0,k1,k2,k3,k4,i0,i1,i2):
                                print "Valid match found."
```

Table 1: Python code to verify G_8 is non-Lombardi

Proof. Let G be formed from a graph G', having at least two degree-one vertices u and v that do not share a common neighbor, by merging u and v and creating a degree-two vertex w. If G is Lombardi, then so is G' as we can take a Lombardi drawing of G, split w, and place u and v on the arcs between w and its respective neighbor, and still maintain a valid Lombardi drawing. Thus, we can take any collection of disjoint copies of G_8 and combine degree-one vertices as described above to form a biconnected non-Lombardi graph. □

4.2 Smooth 2-Lombardi Drawings

If we want to draw Lombardi style drawings for any given graph we have to relax one of the two requirements that specify Lombardi drawings. Ideally, we would like to avoid relaxing the requirement that edges have perfect angular resolution. Fortunately, as the following theorem shows, we can achieve a "close-to-Lombardi" drawing for any graph if we allow two circular arcs per edge.

Theorem 3. *Every graph has a smooth 2-Lombardi drawing. Furthermore, the vertices can be chosen to be in any fixed position.*

Proof. Starting with the given graph G, subdivide every edge by dividing it in two and adding a "dummy" vertex incident to these two new edges. Let G_2 denote the resulting 2-degenerate graph. Duncan et al. [15] show that any 2-degenerate graph has a Lombardi drawing. Furthermore, each dummy vertex of G_2 that was added to subdivide an edge of G has degree 2; hence, in a Lombardi drawing of G_2 the edges incident on each such dummy vertex have tangents that meet at 180 degrees. Thus, when we consider these two circular arcs of G_2 as a single edge of G they define a smooth two-arc edge. See Figure 16(a).

The 2-degenerate drawing algorithm orders the vertices in such a way that each vertex has at most two earlier neighbors; it places vertices with zero or one previous neighbor freely, but vertices with two previous neighbors are constrained to lie on a circular arc. For G_2, we can choose an ordering in which only the dummy vertices have two previous neighbors; therefore, the vertices of G can have any initial placement. □

As Figure 16(b) illustrates, although we can place the vertices in any position with any initial orientation, an arc's smooth bend point might be an inflection point.

5 Planar k-Lombardi Drawings

We have seen that with k-Lombardi drawing we can represent many more graphs than with the standard Lombardi drawing. Planar Lombardi drawings, however are limited to only a subset of the planar graphs. In this section we investigate the combination of planarity and k-Lombardi drawing.[3]

[3] In the conference version [14] of this paper we proved that planar graphs of maximum degree 3 have a planar smooth 2-Lombardi drawing. We dropped this result as in the meantime Eppstein [18] showed that these graphs are actually even planar Lombardi.

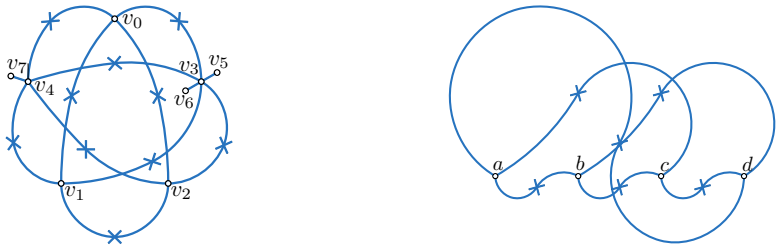

Figure 16: (a) An example 2-Lombardi drawing of G_8. The bend points (not all of which are necessary) are shown with crossed marks. (b) An example 2-Lombardi drawing of K_4 with the vertices placed on a line and tangents oriented to force numerous inflection points.

5.1 Planar 2-Lombardi Pointed Drawings for Planar Graphs

We now show that every planar graph allows a planar 2-Lombardi drawing with pointed joints. The approach is similar to the previous section, but the drawing method inside the disks is different.

Assume that we are given a circle C, a set P of n points on C, and four integers n_1, n_2, n_3, n_4 that sum up to n and that satisfy the inequalities $\lfloor n/4 \rfloor \leq n_i \leq \lceil n/4 \rceil$ and $\lfloor n/2 \rfloor \leq n_i + n_{(i+1) \bmod 4} \leq \lceil n/2 \rceil$. We will show (Lemma 7) that there exist two circles A and B disjoint from P such that A, B, and C are pairwise perpendicular and such that A and B subdivide P into four sets of cardinality n_1, n_2, n_3 and n_4.

It is convenient to begin with a continuous analogue of the lemma. We define a *smooth* probability distribution on C to be a distribution that assigns a nonzero probability to any arc of C, such that arbitrarily short arcs have a probability that approaches zero.

Lemma 6. *Let C be a circle, and Π be a smooth probability distribution on C. Then there exist two circles A and B such that A, B, and C are pairwise perpendicular and such that the four arcs of C formed by its crossing points with A and B each have probability $1/4$ under distribution Π.*

Proof. We may view A and B as arcs inside C (ignoring part of the circles) that end perpendicular to C, and cross each other at a 90° angle. Figure 17(b) illustrates this. We can consider C as a hyperbolic plane in the Poincaré disc model. With this interpretation, A and B represent perpendicular lines in this plane, and C is the set of points at infinity.

Let X be a line that divides C into two arcs that each have probability $1/2$. There exists a (combinatorially) unique line Y perpendicular to X that also divides C into two arcs with probability $1/2$. The four arcs formed by the crossings of C with both X and Y necessarily have probabilities $1/4 + x, 1/4 - x, 1/4 + x, 1/4 - x$ for some x, but it will not necessarily be the case that $x = 0$. Now, we conceptually rotate X and Y, keeping them perpendicular and maintaining invariant the property that each of X and Y divides P into two equal-probability arcs. As we do so, x will change continuously; by the time we rotate X into the position initially occupied by Y, x will have negated its original value. Therefore,

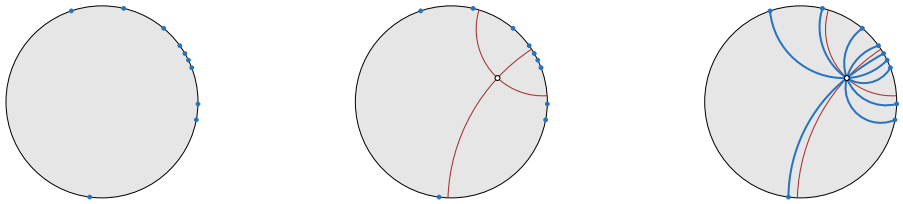

(a) (b) (c)

Figure 17: (a) A disk with a set of connection points on its boundary. (b) A placement for the vertex in the disk that divides the connection points into four quadrants. (c) The actual connections are not fixed, and guaranteed to not intersect.

by the intermediate value theorem, there must be some position during the rotation at which $x = 0$. The circles A and B formed by extending X and Y outside the model of the hyperbolic plane, for this position, satisfy the statement of the lemma. □

Lemma 7. *Let C be a circle, and P be a set of n points on C. Additionally suppose that the four integers n_1, n_2, n_3, n_4 sum up to n and satisfy the inequalities $\lfloor n/4 \rfloor \le n_i \le \lceil n/4 \rceil$ and $\lfloor n/2 \rfloor \le n_i + n_{(i+1) \bmod 4} \le \lceil n/2 \rceil$. Then there exist two circles A and B disjoint from P such that A, B, and C are pairwise perpendicular and such that A and B subdivide P into four sets of cardinality n_1, n_2, n_3 and n_4.*

Proof. For any sufficiently small number ϵ, let Π_ϵ be the smooth probability distribution formed by adding a uniform distribution with total probability ϵ on all of C to a uniform distribution with total probability $1-\epsilon$ on the points within distance ϵ of P. Apply Lemma 6 to Π_ϵ, and let A and B be pairs of circles obtained in the limit as ϵ goes to zero. Then (if points on the boundaries of the arcs are assigned fractionally to the two arcs they bound as appropriate) the number of points assigned to each of the four arcs of C disjoint from A and B is exactly $n/4$.

Next, rotate A and B by a small amount around their crossing point (as hyperbolic lines), that is, preserving their perpendicularity to each other and to C. This rotation causes them to become disjoint from all points in P. Each of the four arcs determined by the four crossing points, and each of the two longer arcs determined by two of the four crossing points, gains or loses only a fractional point by this rotation, so the inequalities $\lfloor n/4 \rfloor \le n_i \le \lceil n/4 \rceil$ and $\lfloor n/2 \rfloor \le n_i + n_{(i+1) \bmod 4} \le \lceil n/2 \rceil$ (where n_i denotes the size of the ith arc) remain true after this rotation. However, there may be more than one solution to this system of inequalities, so we analyze cases according to the value of n modulo four to determine that the solution obtained geometrically in this way matches the values of n_i given to us in the lemma:

- If $n = 0 \pmod 4$, the only choice for the values of n_i is that all of them are equal to $n/4$.
- If $n = 1 \pmod 4$, then three of the n_i must be $\lfloor n/4 \rfloor$ and one must be $\lceil n/4 \rceil$. By exchanging the roles of A and B as necessary we can ensure that the quadrant that is supposed to contain the larger number of points is the one that actually does.

- If $n = 2 \pmod 4$ then the only solution to the inequalities is that two opposite quadrants have $\lfloor n/4 \rfloor$ points and the other two have $\lceil n/4 \rceil$. Again, by exchanging A and B if necessary we can ensure that the correct two quadrants have the larger number of points.

- If $n = 3 \pmod 4$, then one of the n_i must be $\lfloor n/4 \rfloor$ and the remaining three must be $\lceil n/4 \rceil$. Again, by exchanging the roles of A and B as necessary we can ensure that the quadrant that is supposed to contain the smaller number of points is the one that actually does.

Thus, in each case the partition satisfies the requirements of the lemma. □

Now, we apply the lemma to draw the neighborhood of each vertex inside a circle in such a way that their half-edges can be connected into 2-Lombardi edges.

Lemma 8. *Given a circle C and a set P of n points on C, there exists a point p in C such that we can draw n edges from p to the points in P as circular arcs that lie completely inside C, do not cross each other, and meet in p at $360/n^\circ$ angles.*

Proof. Draw n ports around a point with equal angles, and draw two perpendicular lines through the point (not coinciding with any ports), and count the number of points in each quadrant. Let these numbers be $n_1, \ldots, n_4$ and find two circles A and B as in Lemma 7. Then we place p at their intersection point inside C. Now orient the ports at p such that each quadrant has the correct number of ports.

Within any quadrant, there is a circular arc tangent to C at the point where it is crossed by B, and tangent to A at point p; this can be seen by using a Möbius transformation to transform A and B into a pair of perpendicular lines, after which the desired arc has half the radius of C. By the intermediate value theorem, there are two circular arcs from p to any point q on the boundary arc of the quadrant that remain entirely within the quadrant and are tangent to A and B respectively. By a second application of the intermediate value theorem, there is a unique circular arc that connects p to each connection point on the boundary of C, such that the outgoing direction at p matches the port, and such that the arc remains entirely within its quadrant.

Any two arcs that belong to the same quadrant belong to two circles that cross at p and at one more point. Whether that second crossing point is inside or outside of the quadrant can be determined by the relative ordering of the two arcs at p and on the boundary of the quadrant. However, since the ordering of the ports and of the connection points is the same, none of the crossings of these circles are within the quadrant, so no two arcs cross. □

Figure 17(c) illustrates the lemma. We now have all ingredients to prove the main result of this section.

Theorem 4. *Every planar graph has a planar pointed 2-Lombardi drawing.*

Proof. We first obtain a touching-circles representation of a the given graph G using the Koebe–Andreev–Thurston theorem. Each vertex v in G is represented by a circle C; place v together with arcs connecting it to the set of contact points on C using Lemma 8. The arcs meet up at the contact points to form (non-smooth) 2-Lombardi edges. □

5.2 Smooth 3-Lombardi Planar Realization for Planar Graphs

Note that the 2-Lombardi planar realization of the previous section has non-smooth bends in each edge. As we now show, every planar graph also has a smooth 3-Lombardi drawing.

It seems likely that every planar graph G has a smooth 3-Lombardi drawing formed by perturbing each edge of a straight-line drawing of G into a curve formed by two very small circular arcs near each endpoint of the edge, connected to each other by a straight segment. However, the details of this construction are messy. An alternative construction is much simpler, once Theorem 4 is available:

Theorem 5. *Every planar graph has a planar smooth* 3*-Lombardi drawing.*

Proof. Find a pointed planar 2-Lombardi drawing by Theorem 4. For each pointed bend of the drawing formed by two circular arcs a_1 and a_2, replace the bend by a third circular arc tangent to both a_1 and a_2, with the two points of tangency close enough to the bend to avoid crossing any other edge. □

6 Conclusions

We have proven several new results about planarity of Lombardi drawings and about classes of graphs that can be drawn with k-Lombardi drawings rather than Lombardi drawings. However, several problems remain open, including the following:

1. Characterize the subclass of planar graphs that are planar Lombardi. In particular, are all outerplanar graphs planar Lombardi? What is the complexity of testing Lombardi planarity?
2. Characterize the subclass of planar graphs that have smooth 2-Lombardi planar realizations.
3. Address the questions of the area and resolution needed for Lombardi drawings of graphs.
4. Finally, it would be valuable to investigate the readability of the planar and k-Lombardi drawings created by our algorithms, and more specifically, which of our two methods to create smooth 3-Lombardi planar drawings yields visually more pleasing results.

References

[1] Oswin Aichholzer, Wolfgang Aigner, Franz Aurenhammer, Kateřina Čech Dobiášová, Bert Jüttler, and Günter Rote. Triangulations with circular arcs. In M. van Kreveld and B. Speckmann, editors, *Graph Drawing (GD'11)*, volume 7034 of *LNCS*, pages 296–307. Springer, 2012.

[2] Md. Jawaherul Alam, Michael A. Bekos, Michael Kaufmann, Stephen G. Kobourov, Philipp Kindermann, and Alexander Wolff. Smooth orthogonal drawings of planar graphs. In A. Pardo and A. Viola, editors, *Theoretical Informatics (LATIN'14)*, volume 8392 of *LNCS*, pages 144–155. Springer, 2014.

[3] José S. Andrade, Jr., Hans J. Herrmann, Roberto F. S. Andrade, and Luciano R. da Silva. Apollonian networks: Simultaneously scale-free, small world, Euclidean, space filling, and with matching graphs. *Physics Review Letters*, 94:018702, 2005.

[4] Evmorfia Argyriou, Sabine Cornelsen, Henry Förster, Michael Kaufmann, Martin Nöllenburg, Yoshio Okamoto, Chrysanthi Raftopoulou, and Alexander Wolff. Orthogonal and smooth orthogonal layouts of 1-planar graphs with low edge complexity. In T. Biedl and A. Kerren, editors, *Graph Drawing and Network Visualization (GD'18)*, LNCS. Springer, 2018.

[5] Douglas N. Arnold and Jonathan Rogness. Möbius Transformations Revealed. *Notices of the AMS*, 55(10):1226–1231, 2008.

[6] Michael A. Bekos, Henry Förster, and Michael Kaufmann. On smooth orthogonal and octilinear drawings: Relations, complexity and Kandinsky drawings. In F. Frati and K.-L. Ma, editors, *Graph Drawing and Network Visualization (GD'17)*, volume 10692 of *LNCS*, pages 169–183. Springer, 2018.

[7] Michael A. Bekos, Martin Gronemann, Sergey Pupyrev, and Chrysanthi N. Raftopoulou. Perfect smooth orthogonal drawings. In *Information, Intelligence, Systems and Applications (IISA'14)*, pages 76–81, 2014.

[8] Michael A. Bekos, Michael Kaufmann, Stephen G. Kobourov, and Antonios Symvonis. Smooth orthogonal layouts. *J. Graph Algorithms Appl.*, 17(5):575–595, 2013.

[9] Ulrik Brandes and Dorothea Wagner. Using graph layout to visualize train interconnection data. *J. Graph Algorithms Appl.*, 4(3):135–155, 2000.

[10] C. C. Cheng, Christian A. Duncan, Michael T. Goodrich, and Stephen G. Kobourov. Drawing planar graphs with circular arcs. *Discrete Comput. Geom.*, 25(3):405–418, 2001.

[11] Roman Chernobelskiy, Kathryn Cunningham, Michael T. Goodrich, Stephen G. Kobourov, and Lowell Trott. Force-directed Lombardi-style graph drawing. In M. van Kreveld and B. Speckmann, editors, *Graph Drawing (GD'11)*, volume 7034 of *LNCS*, pages 320–331. Springer, 2012.

[12] Giuseppe Di Battista and Luca Vismara. Angles of planar triangular graphs. *SIAM J. Discrete Math.*, 9(3):349–359, 1996.

[13] Matthew Dickerson, David Eppstein, Michael T. Goodrich, and Jeremy Yu Meng. Confluent drawings: Visualizing non-planar diagrams in a planar way. *J. Graph Algorithms Appl.*, 9(1):31–52, 2005.

[14] Christian A. Duncan, David Eppstein, Michael T. Goodrich, Stephen G. Kobourov, and Maarten Löffler. Planar and poly-arc Lombardi drawings. In M. van Kreveld and B. Speckmann, editors, *Graph Drawing (GD'11)*, volume 7034 of *LNCS*, pages 308–319. Springer, 2012.

[15] Christian A. Duncan, David Eppstein, Michael T. Goodrich, Stephen G. Kobourov, and Martin Nöllenburg. Lombardi drawings of graphs. *J. Graph Algorithms and Appl.*, 16(1):85–108, 2012.

[16] Christian A. Duncan, David Eppstein, Michael T. Goodrich, Stephen G. Kobourov, and Martin Nöllenburg. Drawing trees with perfect angular resolution and polynomial area. *Discrete Comput. Geom.*, 49(2):157–182, 2013.

[17] Alon Efrat, Cesim Erten, and Stephen G. Kobourov. Fixed-location circular arc drawing of planar graphs. *J. Graph Algorithms Appl.*, 11(1):145–164, 2007.

[18] David Eppstein. A Möbius-invariant power diagram and its applications to soap bubbles and planar Lombardi drawing. *Discrete Comput. Geom.*, 52:515–550, 2014.

[19] David Eppstein. Simple recognition of Halin graphs and their generalizations. *J. Graph Algorithms Appl.*, 20(2):323–346, 2016.

[20] David Eppstein, Maarten Löffler, Elena Mumford, and Martin Nöllenburg. Optimal 3d angular resolution for low-degree graphs. *J. Graph Algorithms Appl.*, 17(3):173–200, 2013.

[21] Benjamin Finkel and Roberto Tamassia. Curvilinear graph drawing using the force-directed method. In J. Pach, editor, *Graph Drawing (GD'04)*, volume 3383 of *LNCS*, pages 448–453. Springer, 2005.

[22] Ashim Garg and Roberto Tamassia. Planar drawings and angular resolution: Algorithms and bounds. In J. van Leeuwen, editor, *Algorithms (ESA'94)*, volume 855 of *LNCS*, pages 12–23. Springer, 1994.

[23] Michael T. Goodrich and Christopher G. Wagner. A framework for drawing planar graphs with curves and polylines. *J. Algorithms*, 37(2):399–421, 2000.

[24] Carsten Gutwenger and Petra Mutzel. Planar polyline drawings with good angular resolution. In S. Whitesides, editor, *Graph Drawing (GD'98)*, volume 1547 of *LNCS*, pages 167–182. Springer, 1998.

[25] Weidong Huang, Peter Eades, Seok-Hee Hong, and Henry Been-Lirn Duh. Effects of curves on graph perception. In *IEEE Pacific Visualization Symposium (PacificVis'16)*, pages 199–203, 2016.

[26] G. Kant. Drawing planar graphs using the canonical ordering. *Algorithmica*, 16:4–32, 1996.

[27] A. Lhuillier, Christopher Hurter, and Alexandru Telea. State of the art in edge and trail bundling techniques. *Computer Graphics Forum*, 36(3):619–645, 2017.

[28] Mark Lombardi and Robert Hobbs. *Mark Lombardi: Global Networks*. Independent Curators, 2003.

[29] Maarten Löffler and Martin Nöllenburg. Planar Lombardi drawings of outerpaths. In W. Didimo and M. Patrignani, editors, *Graph Drawing (GD'12)*, volume 7704 of *LNCS*, pages 561–562. Springer, 2013.

[30] S. Malitz and A. Papakostas. On the angular resolution of planar graphs. *SIAM J. Discrete Math.*, 7(2):172–183, 1994.

[31] Helen C. Purchase, John Hamer, Martin Nöllenburg, and Stephen G. Kobourov. On the usability of Lombardi graph drawings. In W. Didimo and M. Patrignani, editors, *Graph Drawing (GD'12)*, volume 7704 of *LNCS*, pages 451–462. Springer, 2013.

[32] Kai Xu, Chris Rooney, Peter Passmore, Dong-Han Ham, and Phong H. Nguyen. A user study on curved edges in graph visualization. *IEEE Trans. Visualization and Computer Graphics*, 18(12):2449–2456, 2012.